White Rose Research Online

eprints@whiterose.ac.uk
https://eprints.whiterose.ac.uk
Universities of Leeds, Sheffield and York

Deposited via The University of York.

White Rose Research Online URL for this paper:
https://eprints.whiterose.ac.uk/id/eprint/181669/

Version: Accepted Version

Article:
Zhan, Jiahui, Hu, Rui, Luo, Xi et al. (2021) Highly selective conversion of phenol to cyclohexanol over increased acidity on the Ru/Nb2O5-nC18PA catalysts in biphasic system under mild condition. Green Chemistry. ISSN: 1463-9270

https://doi.org/10.1039/D1GC04046D

Reuse
Items deposited in White Rose Research Online are protected by copyright, with all rights reserved unless indicated otherwise. They may be downloaded and/or printed for private study, or other acts as permitted by national copyright laws. The publisher or other rights holders may allow further reproduction and re-use of the full text version. This is indicated by the licence information on the White Rose Research Online record for the item.

Takedown
If you consider content in White Rose Research Online to be in breach of UK law, please notify us by emailing eprints@whiterose.ac.uk including the URL of the record and the reason for the withdrawal request.

UNIVERSITY OF LEEDS
University of Sheffield
UNIVERSITY of York

Check for updates

View Article Online
View Journal

Green Chemistry

Cutting-edge research for a greener sustainable future

Accepted Manuscript

This article can be cited before page numbers have been issued, to do this please use: J. Zhan, R. Hu, X. Luo, C. Zhang, G. Luo, J. Fan, J. Clark and S. Zhang, *Green Chem.*, 2021, DOI: 10.1039/D1GC04046D.

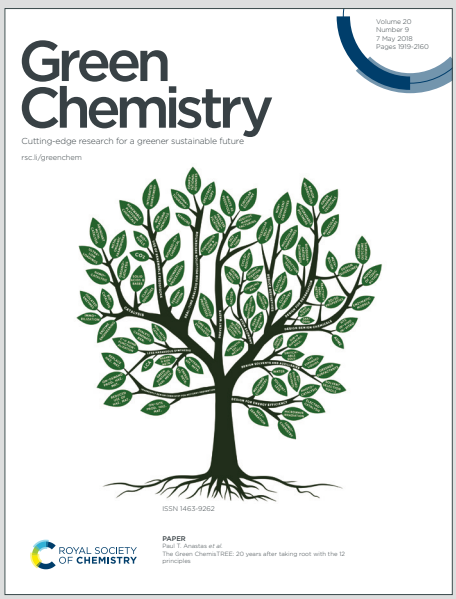

This is an Accepted Manuscript, which has been through the Royal Society of Chemistry peer review process and has been accepted for publication.

Accepted Manuscripts are published online shortly after acceptance, before technical editing, formatting and proof reading. Using this free service, authors can make their results available to the community, in citable form, before we publish the edited article. We will replace this Accepted Manuscript with the edited and formatted Advance Article as soon as it is available.

You can find more information about Accepted Manuscripts in the Information for Authors.

Please note that technical editing may introduce minor changes to the text and/or graphics, which may alter content. The journal's standard Terms & Conditions and the Ethical guidelines still apply. In no event shall the Royal Society of Chemistry be held responsible for any errors or omissions in this Accepted Manuscript or any consequences arising from the use of any information it contains.

Please do not adjust margins

Green Chemistry

View Article Online
DOI: 10.1039/D1GC04046D

PAPER

Highly selective conversion of phenol to cyclohexanol over increased acidity on the Ru/Nb_2O_5-nC18PA catalysts in biphasic system under mild condition†

Received 00th January 20xx,
Accepted 00th January 20xx

DOI: 10.1039/x0xx00000x

rsc.li/greenchem

Jiahui Zhan, [a, b] Rui Hu, [a, b] Xi Luo, [a, b] Cheng Zhang, [c, *] Gang Luo, [a, b] Jiajun Fan, [d] James H. Clark, [a, b, d] and Shicheng Zhang [a, b, *]

Cyclohexanol is an essential intermediate in the chemical industry for the synthesis of nylon and other materials, but the direct hydrogenation of phenol to produce cyclohexanol is problematic due to excessive energy consumption associated with the harsh reaction conditions. In this regard, the novel composite catalysts (Ru/Nb_2O_5-nC18PA) coated with octadecylphosphonic acid (C18PA) was prepared via an impregnation method to be applied for the efficient hydrogenation of phenol to produce cyclohexanol in the biphasic system consisting of water and decalin solvent. Under a hydrogen pressure of 12 bar and 80 °C, nearly 100% conversion of phenol and 93% yield of cyclohexanol are achieved within 4 hours. With the introduction of more Lewis acid sites the aromatic ring is activated which promotes the HYD (hydrogenation) path of phenol, thereby giving an improved selectivity to cyclohexanol. A mechanism exploration experiment was carried out and showed that the strong binding effect between the surface of the Ru/Nb_2O_5-nC18PA catalysts and the benzene ring allows the aromatic ring in phenol to be hydrogenated increasing the selectivity to cyclohexanol. This biphasic catalytic system enhances the potential value of lignin via the catalytic hydrogenation of lignin-derived phenols.

1. Introduction

With the increasing shortage of fossil energy and the gradual deterioration of the global environment there is a growing trend to develop economically renewable raw materials for energy and chemicals from lignocellulosic biomass[1,2]. As one of the main components of lignocellulose, lignin usually exists in the range of 15-30% of dry weight and 40% of energy in plants[3]. Due to the unique structure and chemical properties of aromatic polymers (methoxylated phenylpropane biopolymers), lignin can be catalytically converted into biofuels and chemicals through hydrogenation and hydrodeoxygenation reactions[4,5]. However, the complex chemical structure and high degree of condensation of lignin leads to the production of hundreds of oxygen-containing bio-oil compounds. Among them, phenol is the main bio-oil component[6].

Cyclohexanol, as an indispensable synthetic intermediate for the production of hexamethylene diamine, caprolactam for nylon 6, and adipic acid for nylon 66, is an important commodity in the chemical industry[7,8]. It is a crucial raw material for the preparation of surfactants, detergents and plasticizers and has even greater industrial manufacturing prospects[9,10]. The production of cyclohexanol is mainly carried out through the oxidation of cyclohexane or the hydrogenation of phenol[11,12]. Compared with the hydrogenation of phenol, the oxidation of cyclohexane is almost unfavorable because it requires high temperature and high pressure, low conversion, and is accompanied by a large number of unwanted by-products and other shortcomings[13]. Phenol hydrogenation is an attractive production route and the green technology of choice for the production of cyclohexanol, because such a catalytic system improves atomic efficiency and saves energy[14]. Moreover, the derivatized phenol obtained by the catalytic conversion of lignin undergoes efficient catalytic hydrogenation to produce cyclohexanol, which improves the more valuable resource utilization of lignin, thereby economically and effectively realizing the chemical cycle of lignin[15].

The liquid phase hydrogenation of phenol has attracted considerable interest from researchers[7,16]. It can overcome the catalyst deactivation caused by the agglomeration of metal particles and carbon deposition at high temperatures in the gas phase conditions. The key to the liquid phase hydrogenation of phenol lies in the design of the catalyst and the improvement of product selectivity[17]. Up to now, traditional catalysts have disadvantages such as easy deactivation, blocking of catalyst pores and active sites,

[a] Shanghai Technical Service Platform for Pollution Control and Resource Utilization of Organic Wastes, Shanghai Key Laboratory of Atmospheric Particle Pollution and Prevention (LAP3), Department of Environmental Science and Engineering, Fudan University, Shanghai 200438, China. E-mail: zhangsc@fudan.edu.cn
[b] Shanghai Institute of Pollution Control and Ecological Security, Shanghai, 200092, China.
[c] College of Environmental and Resource Sciences, Zhejiang A&F University, Hangzhou 311300, China. E-mail: success.zhang@zafu.edu.cn
[d] Green Chemistry Centre of Excellence, Department of Chemistry, University of York, York, YO10 5DD, UK.

†Electronic Supplementary Information (ESI) available: XPS spectra in all element and P 2p regions for the Ru/Nb_2O_5-nC18PA catalysts, SEM, TEM images and NH_3-TPD profiles of Ru/Nb_2O_5-nC18PA catalysts, color photograph of the emulsion, additional figures and tables. See DOI: 10.1039/x0xx00000x

Published on 13 December 2021. Downloaded by University of York on 12/15/2021 10:04:11 AM.

Green Chemistry Accepted Manuscript

View Article Online DOI: 10.1039/D1GC04046B

Published on 13 December 2021. Downloaded by University of York on 12/15/2021 10:04:11 AM.

and easy sintering of active metals, resulting in a significant decrease in catalytic activity[18]. Here, noble metal catalysts including Ru[19] and Pt[20] etc. supported composite materials have broken the shackles of traditional catalysts and are widely used in the hydrogenation of phenol and its phenolic compounds. Nevertheless, the reaction process still needs to be carried out under harsh conditions (and greater than 100°C and/or 15 bar H_2), making excessive energy consumption detrimental to sustainable development[9,21,22]. For instance, Tan et al.[7] studied the Pd/NaY catalysts for phenol hydrogenation in ethanol at 235°C and 5 MPa H_2. The conversion of phenol was 78.2%, and the selectivity to cyclohexanol was 92.3%. Vladimir et al.[23] developed the Core/Shell Ruthenium-Halloysite nanocomposite materials to achieve complete conversion of phenol in an aqueous solution of 3 MPa H_2 at 80°C and a 100% yield of cyclohexanol. Therefore, there is an urgent need to develop noble catalysts to achieve efficient and green hydrogenation of phenol under mild conditions.

To achieve high reactivity, bifunctional catalysts with metal and acid sites are often used, where hydrogenation occurs mainly at the metal site and dehydration and hydrolysis occur at the acid site[24]. It is reported that the supported Ru-based catalysts are superior to other noble metal catalysts due to their moderate cost and high catalytic activity[25,26]. Furthermore, the unique reactivity exhibited by emerging niobium-based catalysts as supports has gained much attention in the depolymerization of lignin and the hydrogenation of lignin derivatives[27]. However, common solid acid catalysts such as zeolites[28], TiO_2[29] and Al_2O_3[30] etc. have high abundance and unique chemical properties in hydrothermal environments but are often accompanied by structural changes in water that trigger catalyst deactivation. In this case, the hydrophobic surface modification of the support can be performed by introducing organic ligands, which not only stabilizes the catalyst structure inhibiting catalyst deactivation, but also modifies the support surface in a controlled manner while maintaining the intrinsic structure of the support[31]. Among them, the introduction of alkyl phosphonates is a promising approach. The application of alkyl phosphonates in metal oxide supports has been reported to enhance the catalyst activity and improve the structural stability of the catalyst introducing acidic sites[30]. Therefore, we decided that the phosphonic acid can bind to the oxide support and form strong chemical bonds on the surface after deposition onto the catalyst surface[32]. The coated catalyst can improve the selectivity of aryl substituted alcohols, the reaction activity, and slow down the deactivation efficiency of the catalyst[33]. They can also modulate the wettability of the catalyst surface and make it hydrophobic. Meanwhile, a biphasic catalytic system with a solid catalyst stabilized by a particle-stabilized Pickering emulsion as the reaction interface promotes efficient conversion and enables clean separation and catalyst reuse[34]. In addition, among organic solvents, decalin has a wide application potential due to its good hydrogen storage capacity, extraction capacity, and easy recovery[34,35].

This research has developed a novel of acidity increasing composite catalysts (Ru/Nb_2O_5-nC18PA). The unique hydrogenation reaction of phenol was promoted by a synergistic effect between the active metal ruthenium and the Nb_2O_5-nC18PA composite support, in which the C18PA was deposited on the surface of Nb_2O_5. The acid content in the catalyst was substantially increased by depositing C18PA on Ru/Nb_2O_5 catalysts, and the introduction of Brønsted acid sites and a higher number of Lewis acid sites promoted the catalyst activity. Comprehensive characterization was performed to construct a relationship between Ru/Nb_2O_5-nC18PA catalysts and cyclohexanol selectivity. It is worth noting that the reaction can give an ultra-high yield of cyclohexanol at low temperature and low pressure. It is straightforward to separate the product from the catalyst-oil-water biphase, and the catalyst is also used repeatedly. The catalytic system has great industrial application potential and provides a method for the efficient resource utilization of lignin.

2. Experimental

2.1 Materials

Phenol (≥ 99%), decalin (≥ 99.5%) and niobium pentoxide (4N) were supplied by Sinopharm Chemical Reagent Co., Ltd. Benzene (≥ 99.9%), cyclohexanol (≥ 99.0%), cyclohexanone (≥ 99.5%), cyclohexane (≥ 99.5%) and Dodecane (≥ 99.5%) were brought from Aladdin Reagent Corporation. ruthenium acetylacetonate [$Ru(acac)_3$, 97%] and octadecylphosphonic acid (C18PA, 97%) were purchased from Shanghai Macklin Biochemical Co., Ltd. All these reagents were used without further purification.

2.2 Synthesis of the catalysts

The synthesized catalysts refer to our previous preparation methods[36]. The niobium pentoxide was impregnated with a $Ru(acac)_3$ solution containing 1wt.% Ru supported. The impregnated sample was kept at room temperature for 24 h, after which it was rotary evaporated and dried in vacuum at 60°C for 6 h. Finally, it was calcined in a tube furnace with a heating rate of 2 °C/min at 200 °C in an air atmosphere for 2 h, the RuO_x/Nb_2O_5 catalyst was obtained.

The RuO_x/Nb_2O_5 catalyst was immersed in a C18PA solution in methanol in accordance with the total amount of C18PA to form a monolayer on the surface of the support by 30%, 60%, 80%, 100% and 120%. After stirring at 50°C for 16 hours, the mixture was centrifuged to remove the methanol supernatant to obtain a RuO_x/Nb_2O_5-nC18PA catalyst. The n in RuO_x/Nb_2O_5-nC18PA indicate the specific amount of C18PA loaded into the catalyst. For example, to prepare RuO_x/Nb_2O_5-100C18PA catalyst (i.e., the load of C18PA is 100% and n is 100), 1g RuO_x/Nb_2O_5 catalyst needs to be added to 0.50 mM C18PA solution in methanol. Finally, the RuO_x/Nb_2O_5-nC18PA catalyst was annealed at 200°C for 2h at a heating rate of 2°C/min in an air atmosphere, and reduced with the same heating rate at 200°C in a H_2 flow at 3 h to obtain the Ru/ Nb_2O_5-nC18PA catalyst. In addition, the RuO_x/Nb_2O_5 catalyst was calcined in an air atmosphere at 200°C in the previous step for 4 h, and then reduced at 200°C in a H_2 flow for 3 h to obtain the Ru/ Nb_2O_5 catalyst.

We used Inductively Coupled Plasma Atomic Emission Spectroscopy (ICP-MS) to determine the Ru content of the catalysts, and they were close to 1.0 wt. %.

2.3 Characterization of catalyst

Morphology observation and analysis. The morphology and crystal size of the support, the distribution and particle size of ruthenium on the support were analyzed by the Nova NanoSem 450 Scanning Electron Microscope (SEM) of FEI Company in the United States, Tecnai G2 F20 S-Twin Transmission Electron Microscope (TEM) and

Green Chemistry Accepted Manuscript

 This journal is © The Royal Society of Chemistry 20xx

View Article Online
DOI: 10.1039/D1GC04045D

Published on 13 December 2021. Downloaded by University of York on 12/15/2021 10:04:11 AM.

X-Max 80T spectrometer from Oxford Instruments company. The specific sample preparation method is as follows: The powder samples were evenly coated on the black conductive glue, and then placed on the sample table for scanning electron microscope observation. The samples were dispersed on the lacy carbon copper grids for transmission electron microscopy analysis.

Phase structure analysis. The X-ray powder diffraction (XRD) patterns were acquired on the Bruker Advance D8 powder X-ray diffractometer equipped with Cu-Kα radiation. The crystal structures of the catalysts were measured between 10° and 90° with a scan rate of 5°min^{-1}. The Quantachrome Autosorb-iQ2 automatic gas adsorption analyzer was used to analyze the specific surface area of the catalyst, and the fit was performed by the Brunauer-Emmett-Teller (BET) method.

Element Valence Analysis. The X-ray photoelectron spectroscopy (XPS) analysis was performed using Thermo Scientific K-Alpha X-ray photoelectron spectrometer to analyze the state of the catalysst. The binding energy (BE) reference was obtained by using the 284.8 eV C 1s peak.

Surface functional group analysis. The functional groups in all catalysts were measured by Thermo Scientific Nicolet iS5 Fourier Transform Infrared (FTIR) spectrometer in the wavelength range of 400-4000 cm^{-1}.

Surface acid site analysis. The temperature-programmed desorption of ammonia (NH_3-TPD) was used to investigate the acidic properties of the catalysts on a TP 5080 (Tianjin Xianquan) analyzer equipped with a thermal conductivity detector (TCD). The samples (50 mg) were pretreated in the nitrogen atmosphere of 30 mL min^{-1} at 200°C for 0.5h to clean the surface. After cooling the sample to 50°C, the catalysts were exposed to flowing 10% NH_3 in a nitrogen gas mixture (30 mL min $^{-1}$) at 50°C for 1 h. The physically adsorbed and residual NH_3 were removed by purging the catalysts with flowing N_2 at 50°C for 1 h. Then, the catalysts were heated to 800°C in the nitrogen atmosphere at a rate of 10°C min $^{-1}$. The Bruker Tensor 27 infrared spectrometer was used to carry out the pyridine Fourier transform infrared (Py-FT-IR) test of the prepared catalyst to determine the acid type, acid amount and acidity of the catalysts surface.

Wetting performance analysis. The JY-82 contact angle measuring instrument was used to test the catalyst contact angle at room temperature. After the sample was pressed into a sheet and placed on the sample pan to measure the contact angle of water. The water droplets were introduced by the micro-injector. When a water droplet contacted the catalyst on the surface of the sample disk, immediately used a charge-coupled device camera to take photos, and then the angle of the liquid solid interface was measured and determined.

2.4 Hydrodeoxygenation of phenol

Phenol was catalytically converted in a 25mL Hastelloy reactor. In a typical phenol reaction experiment, 0.05 g phenol and 0.05 g catalysts were added to a 10 mL mixed solution of water and decalin in the reactor. The reactor was purged with hydrogen 5 times to exhaust excess air and maintained the hydrogen pressure of 12 bar at room temperature while stirring at 700 rpm, and the reactor was heated to 80°C. After the catalytic reaction was completed, the reactor was placed in a water tank and quickly cooled to ambient temperature. A filter equipped with an organic membrane was used to separate the solid and liquid phases. Then the resulting layered liquid was separated into the aqueous phase and the organic phase. Finally, the analyzed samples were filtered through 0.22 μm filters, and then the samples of each phase were analyzed through GC-MS and GC-FID.

The following definitions calculated the conversion of phenol, the selectivity and yield of each product:

Conversion (%) = (moles of carbon in reactant involved (mol)) / (moles of carbon in inital reactant (mol)) × 100 (1)

Selectivity (%) = (moles of carbon in the product (mol)) / (total of moles of carbon in all products (mol)) × 100 (2)

Yield (%) = Conversion (%) × Selectivity (%) ÷ 100 (3)

3. Results and discussion

3.1 Characterization of the catalysts

3.1.1 XRD. The XRD patterns of all fresh catalysts are shown in Fig. 1. The diffraction peaks at 2θ = 23.7, 24.8, 25.4, 32.1, 35.3, 38.9, 44.3, 47.6, 51.0, 54.3, 60.5, 64.0, 66.9, 72.2° of Ru/Nb_2O_5-nC18PA catalysts with different loadings correspond to (-513), (121), (-604), (314), (-812), (-518), (-809), (-1113), (-1010), (336), (050), (15-4), (551), (1034) monoclinic Nb_2O_5 phase (JCPDS 19-0862)[37]. In addition, the figure does not show the diffraction peak attributed to the metallic Ru phase, which may be due to the low Ru loading (1 wt.%) or the Ru particles are too small and well dispersed on the supports, which is consistent with the HRTEM image (Fig. 4). Among them, Ru (101) coincides with Nb_2O_5(-809), which cannot be used as the basis for the judgment of a Ru peak. Moreover, the X-ray spectra before and after loading C18PA and the standard spectrum of Nb_2O_5 show that no new phase is formed after C18PA loading, indicating that the loading of C18PA has no detectable effect on the overall structure of the support.

3.1.2 XPS. The XPS characterization is shown in the Fig. 2. Using the C 1s-Ru 3d core energy level spectrum, the chemical valence states of ruthenium are shown. The binding energy at ~284.3 eV is characteristic of un-reacted/metallic Ru^0, and the binding energy at ~285.1 eV is attributed to the reacted Ru^{4+} species, most likely in the form of RuO_2[38,39]. Among them, Ru/Nb_2O_5, and Ru/Nb_2O_5-nC18PA

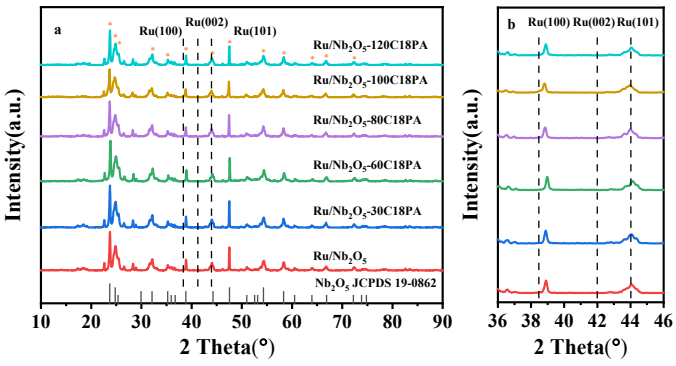

Fig.1 X-Ray diffraction pattern of the Ru/Nb_2O_5-nC18PA catalysts (a). Zoom on the Ru (100), Ru (002) and Ru (101) diffraction peak zone from 36 to 46 degree (b).

Green Chemistry Accepted Manuscript

View Article Online DOI: 10.1039/D1GC04046D

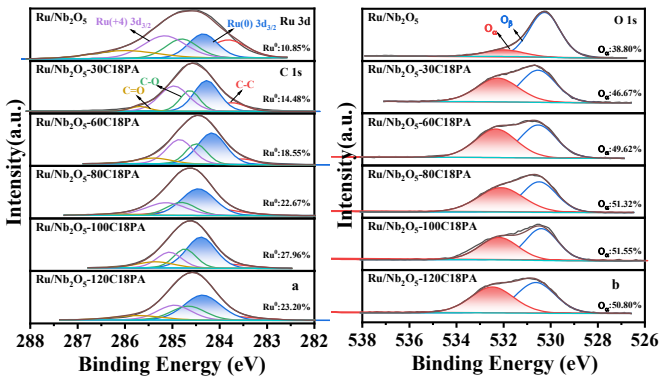

Fig.2 XPS spectra of the Ru/Nb_2O_5-nC18PA catalysts in the C 1s–Ru 3d (a) and O 1s (b) regions.

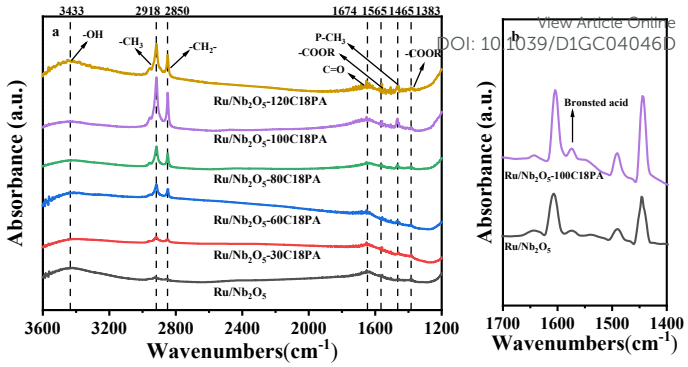

Fig.3 FTIR (a) and pyridine FTIR (b) spectra for the Ru/Nb_2O_5-nC18PA catalysts.

loaded with 30%, 60%, 80%, 100% and 120% C18PA, the ratio of Ru^0/(Ru^0 + Ru^{4+}) is approximately 10.85%, 14.48%, 18.55%, 22.67%, 27.96% and 23.20%, which indicates that the Ru/Nb_2O_5-nC18PA catalyst loaded with 100% C18PA has more metal Ru nanoparticles on the surface, and the TEM observation also shows the same result. Moreover, the O 1s spectra of these composite catalysts also show apparent differences. The peaks at ~530.4eV originate from lattice oxygen (O^{2-}, O_β), while those at ~532.3eV can be assigned to oxygen vacancies (O/OH, O_α). Generally, the ratio of O_α / (O_α + O_β) is used to evaluate the content of oxygen vacancies[40,41]. As shown in the Fig. 2b, the highest oxygen vacancy content reaches 51.55% for Ru/Nb_2O_5-100C18PA among all catalysts, indicating that the oxygen defect concentration on its surface is higher than other catalysts. These Ru oxidation peaks (O^{2-}, O_β) further demonstrate a large amount of Ru oxides, which may be oxidized or not completely oxidized after reduction. It is a remarkable fact that the surface adsorbed oxygen has a better migration ability than the lattice oxygen, so the catalyst with high surface adsorbed oxygen exhibits higher catalytic activity for the selective oxidation of cyclohexanol. Moreover, the electronic effect also largely affects the adsorption strength of the benzene ring and or O-containing functional groups in the phenol on the catalyst. Compared with electron-rich sites, benzene rings may preferentially adsorb on electron-deficient metal sites, which is conducive to the hydrogenation of benzene rings in phenol[42,43].

3.1.3 FTIR. The Fourier transform infrared (FTIR) spectra are showed in Fig. 3. The broad absorption peak at 3433 cm^{-1} belongs to the stretching vibration of hydroxyl (-OH), which mostly is made of surface hydroxyl groups on niobium oxide and C18PA. 2918cm^{-1} and 2850cm^{-1} are attributed to the stretching of the methyl and methylene C-H in the organic phosphonic acid. The P-CH_3 stretching vibration exists at 1465cm^{-1}, indicating that the functionality of the deposited phosphonic acid remains in the organic monolayer. It also shows that the phosphate ester exists in the tail of the alkyl group[31,44], and the relatively high frequency of asymmetric -CH_2 bands indicates a considerable degree of disorder. The disorder of high-frequency asymmetric -CH_2 has been proved in the literature to be consistent with the lack of coordination between phosphonic acid and the support, indicating that the head group of C18PA has Brønsted acidity[45]. In addition, the peak intensity of methyl and methylene groups gradually increase with increasing phosphonic acid loading, and the peak intensity is the strongest when the loading of C18PA is 100%, which is accordance with the catalytic activity of the catalyst in phenol conversion. The following Fourier transform infrared (Py-FT-IR) spectra after pyridine adsorption also support the successful introduction of Brønsted acid (Fig. 3b). Moreover, the introduced Brønsted acidity shows that the P-OH group is retained when the phosphonic acid is bound to the Nb_2O_5 support. This is consistent with the XPS analysis, that is, the peak of the phosphorus 2p binding energy on the phosphonic acid supported catalyst is 133.8 eV, which is assigned to the phosphorus that retains a hydroxyl group. 1674cm^{-1}, 1565cm^{-1} and 1383cm^{-1} are the stretching vibrations of C=O and -COOR groups. These surface functional groups are hydrophilic and lipophilic[46,47], which can adjust the hydrophilic and lipophilic properties of the support.

3.1.4 SEM and TEM. The microstructure and morphology of the Ru/Nb_2O_5-100C18PA catalyst were selected to be characterized and analysed using scanning electron microscopy (SEM) and transmission electron microscopy (TEM). The SEM image (Fig. 4a and 4b) shows that C18PA is deposited on the mesoporous Nb_2O_5 support. In Fig. S2, Ru/Nb_2O_5 intuitively presents a pore-like structure. With increasing C18PA loading the surface of Nb_2O_5 support shows more and more apparent agglomeration of C18PA, which gradually reduces the specific catalyst surface area, as is evident from the BET results (Table S4). The TEM image and its particle size distribution are shown in Fig. 4a and 4b. The average particle size of Ru is 2.0 nm, which indicates that the Ru particles are very uniformly dispersed on the Nb_2O_5 support, which is in good agreement with the XRD observation results (Fig.1). The results of the EDS-mapping analysis further reveals the uniform distribution of P, C and O, confirming the successful loading of C18PA (Fig. 4e). It is worth noting that in the TEM image of the Ru/Nb_2O_5-nC18PA catalysts (Fig. S2), it is clear that the agglomeration of Ru particles is significantly weakened, and the average particle size of Ru gradually decreases (Fig. S3, Table S5). Among them, the Ru/ Nb_2O_5-100C18PA catalyst has the smallest average particle size of ruthenium particles of 2.00 nm, which is consistent with the yield of cyclohexanol in the phenol hydrogenation reaction of the Ru/Nb_2O_5-nC18PA catalysts. In other words, the Ru/Nb_2O_5-100C18PA catalyst has the best catalytic effect and this can be closely related to the dispersion of Ru particles and active sites.

3.2 Catalytic system

Published on 13 December 2021. Downloaded by University of York on 12/15/2021 10:04:11 AM.

Green Chemistry Accepted Manuscript

This journal is © The Royal Society of Chemistry 20xx

Please do not adjust margins

View Article Online
DOI: 10.1039/D1GC04046D

Published on 13 December 2021. Downloaded by University of York on 12/15/2021 10:04:11 AM.

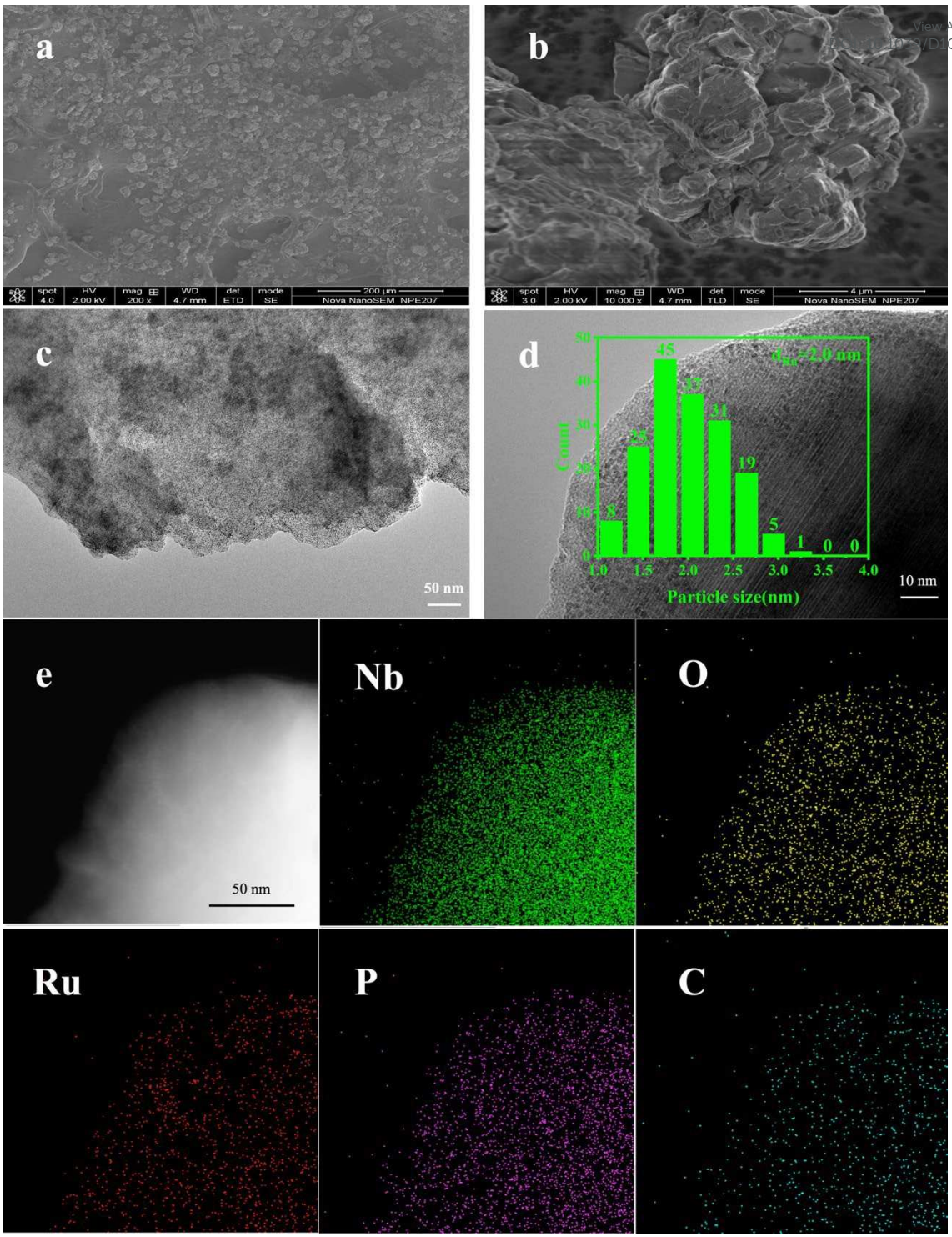

Fig.4 Typical SEM images (a and b) and TEM images (c and d) of the Ru/Nb_2O_5-100C18PA catalyst. Inset (d) the Ru nanoparticle size distributions and EDS-mapping images of the catalyst (e)

3.2.1 The influence of C18PA loading. In a relatively mild biphasic solvent system (200℃), different proportions of C18PA were loaded under conditions that keep the Nb_2O_5 support constant. and the HDO activity of Ru catalyst on the Nb_2O_5, C18PA and Nb_2O_5-nC18PA composite support were further studied. As shown in Fig. 5, the HDO reaction of phenol followed the HYD (hydrogenation) and the DDO (direct deoxygenation) pathway, including the production of cyclohexanol in the HYD and the production of benzene in the DDO. It was observed that the conversion of Ru on the bare Nb_2O_5 support was higher than the conversion of Ru on the Nb_2O_5-nC18PA composite support catalysts, but the selectivity to benzene and cyclohexanol was the lowest. This may be due to the fact that the

Green Chemistry Accepted Manuscript

View Article Online
DOI: 10.1039/D1GC04045D

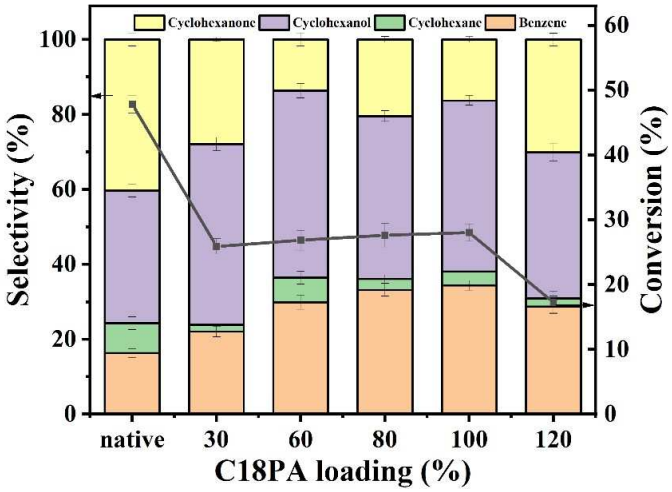

Fig.5 Conversion, selectivity to cyclohexanol, cyclohexanone and benzene for the HDO of phenol at 200 °C, 10 bar H_2 for 4 h over the Ru/Nb_2O_5-nC18PA catalysts with different C18PA loading.

hydrophilic Ru/Nb_2O_5 catalyst has maximum contact in the aqueous phase with higher phenol solubility, and the resulting product has much higher solubility in the decalin phase, corresponding to the extraction process. The latter is caused by the increased hydrophobicity resulting in less contact with phenol, which is mainly present in the aqueous phase. Previous research work has shown that the appearance of benzene may be caused via the Brønsted acid of Ru/Nb_2O_5 and Ru/Nb_2O_5-nC18PA catalysts by means of promoting the dehydration of cyclohexanol at higher temperatures[36]. At the same time, the incompletely coordinated Nb^{5+} cations (ie Lewis acid sites) in the Ru/ Nb_2O_5-nC18PA catalyst are oxygenophilic and can adsorb oxygen atoms on the benzene ring to reduce the energy of C-O bond. In this way the phenol could undergo hydrogenolysis by breaking the $C_{sp}{}^2$–O bond via the DDO pathway. However, the Lewis acid site also has the ability to activate the aromatic ring[48,49], which can lead to hydrosaturation of the aromatic ring, causing the phenol to follow simultaneously and HYD path to generate cyclohexanol. Therefore, it is necessary to control Brønsted acid sites and Lewis acid sites to maximize the selectivity of formation of cyclohexanol.

3.2.2 The relationship between acidic sites and cyclohexanol selectivity. To further reveal the influence of different acid sites on the catalysts for the selective formation of cyclohexanol, we used

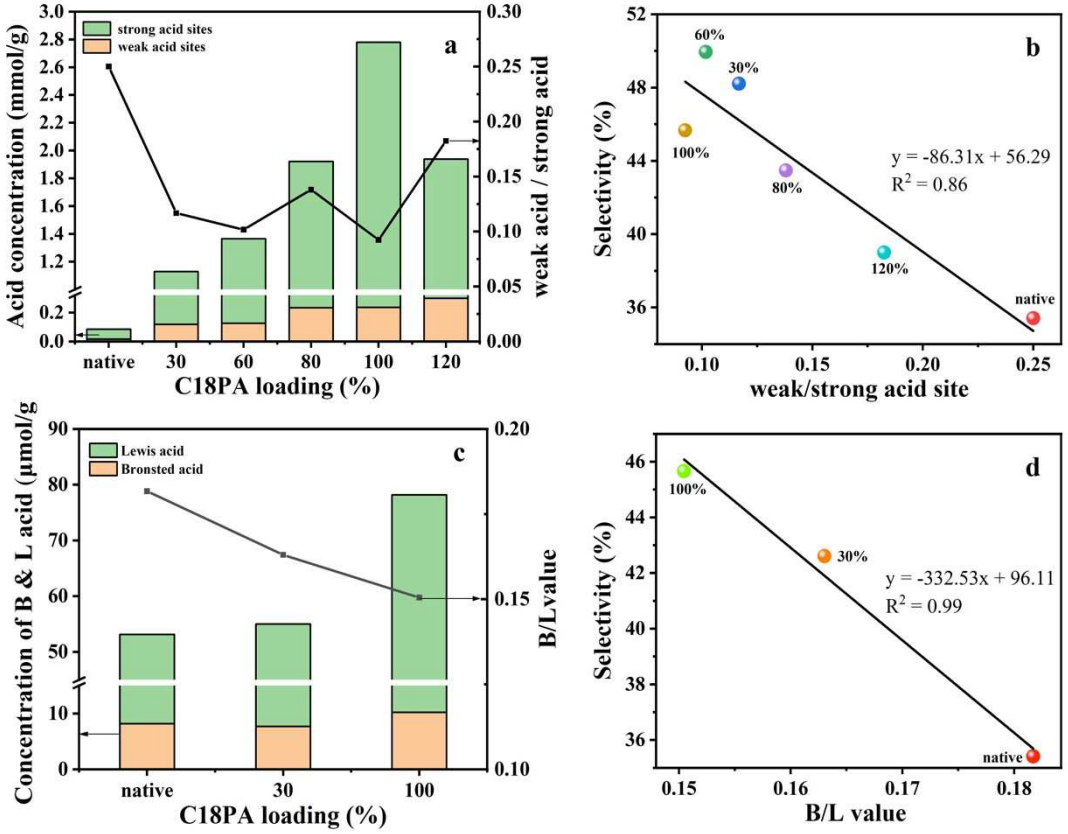

Fig.6 Acid concentration and the ratio of weak to strong acid of Ru/Nb_2O_5-nC18PA catalysts calculated from NH_3-TPD profiles (a), regression analysis between weak/strong acid site and selectivity of cyclohexanol (b), Brønsted acid and Lewis acid concentration, and the ratio of weak to strong acid of Ru/Nb_2O_5-nC18PA catalysts calculated from Py-FT-IR profiles (c), regression analysis between B/L value and selectivity of cyclohexanol (d).

This journal is © The Royal Society of Chemistry 20xx

Published on 13 December 2021. Downloaded by University of York on 12/15/2021 10:04:11 AM.

Green Chemistry Accepted Manuscript

View Article Online
DOI: 10.1039/D1GC04046D

Published on 13 December 2021. Downloaded by University of York on 12/15/2021 10:04:11 AM.

NH_3-TPD to measure the strength of the catalyst acid sites (Fig. 6a). When C18PA was deposited on native Ru/Nb_2O_5 supports, the concentration of weak acid sites and strong acid sites in the catalyst increased significantly, and the latter increased even more. We further selected the native Ru/Nb_2O_5, Ru/Nb_2O_5-30C18PA and Ru/Nb_2O_5-100C18PA catalysts and confirmed the concentrations of Brønsted acid and Lewis acid through the Py-FT-IR test (Fig. 6c), and found that the trend was similar to Fig. 6: the introduction of C18PA increased the Brønsted acid and Lewis acid concentration in the catalyst, and the Lewis acid concentration increased significantly. This may be due to the OH and P=O in C18PA binding to the support during the deposition process. The formation of O-Nb-O-P bonds[50] (Fig. S6) and the binding of H in C18PA to O in Nb_2O_5 would result in an increase of incompletely coordinated Nb^{5+} on the support thus forming more oxygenophilic sites[51,52], i.e., an increase of Lewis acid sites[53]. At the same time, there is a small increase of Brønsted acid because only a small fraction of OH is retained by C18PA after binding to the support.

We quantified the acid sites and performed regression analysis on the ratio of weak acid to strong acid (weak / strong acid value) and found that they have a certain linear relationship with selectivity towards cyclohexanol formation (Fig. 6b). In addition, the regression analysis of the ratio of Brønsted acid to Lewis acid (B/L value) and cyclohexanol selectivity in Fig. 6c has a high linear fitting effect, which further confirms the close relationship between the acid sites and the selectivity to cyclohexanol (Fig. 6d). This is similar to the linear relationship that Xu et al.[38] choose the B/L value of the Ru-WO_x/ZrO_2 catalysts in the HDO of guaiacol as a measure of catalyst selectivity and acidity characteristics. The linear relationship in Fig. 6b and Fig. 6d reveals a positive correlation between Lewis acid sites whereas Brønsted acid sites are negatively correlated with the selectivity to cyclohexanol. Interestingly, the study by J. Will Medlin et al.[31–33] demonstrated that the introduced Brønsted acidity is related to the activity of deoxygenation (DO) when C18PA are deposited on the surface of Pd/Al_2O_3. This is consistent with the negative correlation between Brønsted acid sites and cyclohexanol selectivity. We deposited C18PA on the Ru/Nb_2O_5 catalysts, introducing more Lewis acid sites, so that the selectivity to cyclohexanol will be maximised. This might be due to the higher Lewis acidity dominated by the simultaneous presence of Brønsted acid and Lewis acid sites which is mainly to stimulate the aromatic ring and promote the HYD path to phenol, thereby enabling a higher selectivity to cyclohexanol.

Moreover, the differences in selectivity of products over the Ru/Nb_2O_5-nC18PA catalysts with different C18PA loadings with similar Ru dispersion degree (obtained by characterization) indicates the influence of electron density on hydrogenation activity. The metallic Ru observed in the XPS diagram is advantageous to the hydrogenation of the benzene ring in the phenolic monomer to produce cyclohexanol[54]. This may be due to the different acidic sites on different supports that change the electronic properties of the metal ruthenium center[31,55], making the selection to cyclohexanol in the reaction show the same trend, while Ru/Nb_2O_5 contains more positively charged ruthenium, therefore the selectivity of cyclohexanol is relatively low. Based on the above results, Ru/Nb_2O_5-100C18PA is selected as the preferred catalyst.

3.2.3 The relationship between catalysts wettability and cyclohexanol selectivity. The contact angles of Ru/Nb_2O_5-nC18PA catalysts with different loading ratios of C18PA were measured so as to explore the wettability of the catalysts. The results are shown in Table S5. It was found that the native Ru/Nb_2O_5 catalyst has good hydrophilicity and the contact angle is almost zero. However, the contact angle of the catalyst with C18PA is between 100-108°, suggesting strong amphiphilic properties. In the oil-water biphase, the wettability of the catalyst is the key to the formation of a Pickering emulsion[56]. As expected, the difference in wettability results in different catalyst activity and selectivity. We have found that the wettability of the Ru/Nb_2O_5-nC18PA catalysts have a good linear relationship with the selectivity to cyclohexanol (Fig. 7). This may be due to the catalyst with moderate oil-water wettability, "staying" well on the oil-water interface, thereby stabilizing the Pickering emulsion[30].

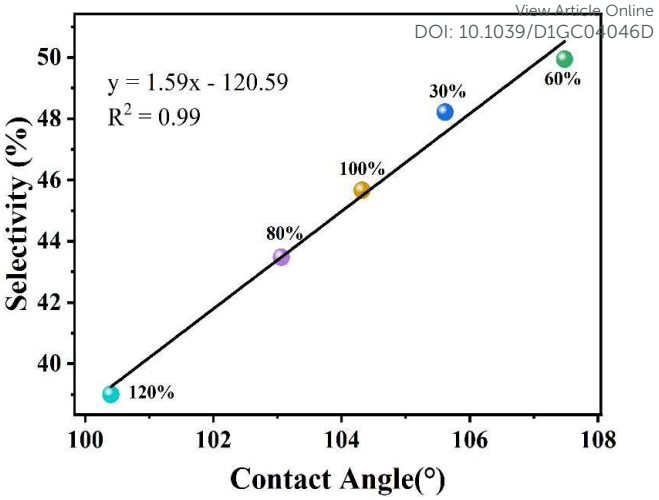

Fig.7 Regression analysis between contact angle and cyclohexanol selectivity for Ru/Nb_2O_5-nC18PA catalysts.

3.3 Catalytic performance

3.3.1 Influence of hydrogen pressure. The hydrogen pressure has a very prominent effect on the catalytic activity of phenol HDO. As shown in Fig. 8a, without hydrogen, the conversion of phenol is almost zero and no reaction occurs. On the contrary, the Ru/Nb_2O_5-100C18PA catalyst has favorable catalytic activity for HDO of phenol in a hydrogen atmosphere under mild conditions. Phenol has been efficiently converted as the hydrogen pressure increases from 2 bar to 12 bar. At the same time, cyclohexanol also reaches its highest value, and remains essentially unchanged as the hydrogen pressure further increases. However, after reaching the peak, the yield of cyclohexanone gradually decreases with increasing hydrogen pressure until it almost disappears. The results reveal that cyclohexanone is an intermediate product of phenol conversion, and was subsequently hydrogenated to form cyclohexanol. The yield of benzene gradually increases as the hydrogen pressure increases. After the hydrogen pressure reaches 10 bar, it decreases with increasing hydrogen pressure. These results indicate that the DDO and HYD of phenol occurred simultaneously at lower hydrogen pressure, and higher hydrogen pressure is conducive to the formation of cyclohexanol. Our results are consistent with the influence of hydrogen pressure on phenol HDO as reported in the literature. Higher hydrogen pressure is beneficial to the

Green Chemistry Accepted Manuscript

View Article Online
DOI: 10.1039/D1GC04046D

Published on 13 December 2021. Downloaded by University of York on 12/15/2021 10:04:11 AM.

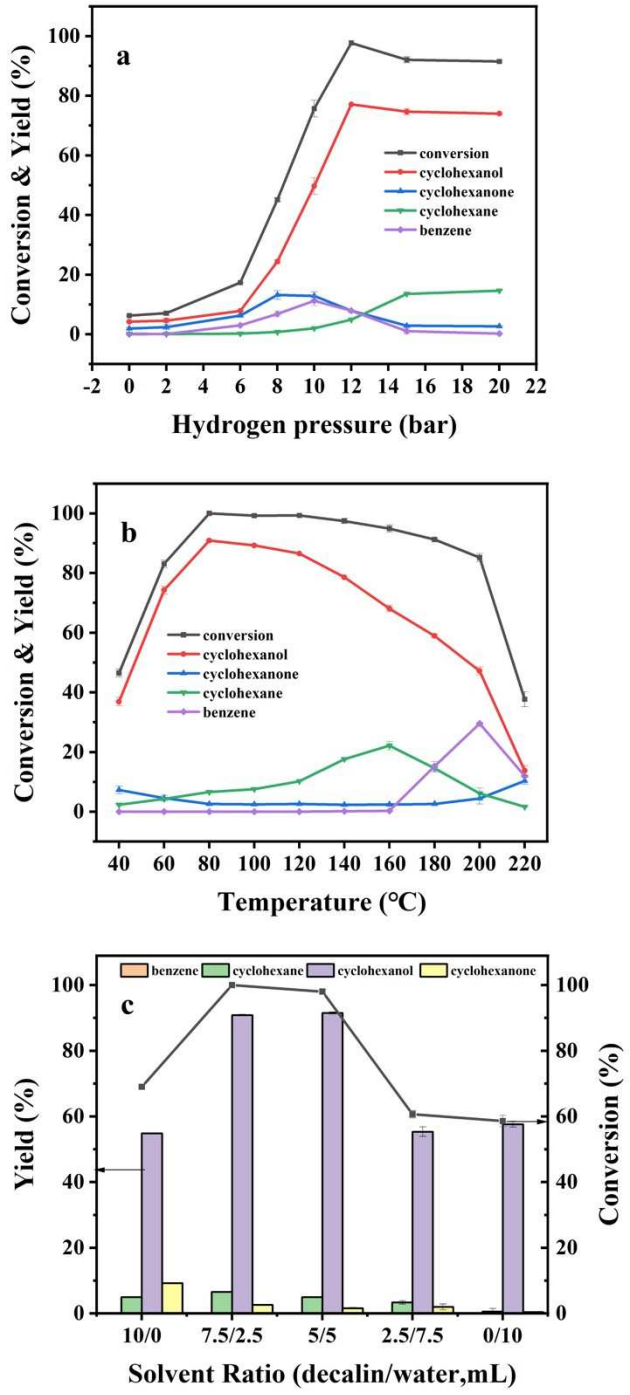

Fig.8 Influence of reaction parameters for the hydrogenation of phenol over the Ru/Nb_2O_5-100C18PA catalyst. Reaction conditions: Phenol (0.05 g), Ru/Nb_2O_5-100C18PA (0.05 g), decalin/water = 7.5 mL/ 2.5 mL, 4 h. 180 °C (a). 12 bar H_2 (b). 80 °C, 12 bar (c).

hydrogenation of phenol rather than deoxygenation[6,16]. As the hydrogen pressure increases, more H_2 can be dissolved in the solvent, thereby promoting the hydrogenation of phenol[7,38].

3.3.2 Influence of reaction temperature. Fig. 8b shows a significant change in phenol and the associated product selectivity with increasing temperature using Ru/Nb_2O_5-100C18PA catalyst. In the lower temperature range (40℃-80℃), phenol gradually undergoes almost complete HDO conversion, and the selectivity to cyclohexanol also reaches the highest value. However, when the temperature is increased, the conversion of phenol and the selectivity to cyclohexanol gradually decrease, accompanied by the production of benzene. This demonstrates that the HDO of phenol mainly produces cyclohexanol, which follows the benzene ring hydrogenation in the HYD path at low temperature. When the temperature rises, the cyclohexanol produced from the phenol in the HYD path is deoxygenated to produce cyclohexane, and the hydrogenation reaction is inhibited[57]. As the HDO of phenol began to appear, the DDO path accompanied by the production of benzene, gradually became dominant as the temperature increased. In summary, low temperature is conducive to the formation of cyclohexanol with few by-products. The lower temperature may not reach the energy of Caryl-OH bond and C_{alkyl}-OH bond cleavage, thereby inhibiting deoxidation[6]. Therefore, the conversion of phenol to cyclohexanol needs to be carried out at a low temperature.

3.3.3 Influence of the ratio of decalin/water on the biphasic catalytic process. The effect of the ratio of decalin/water on the product distribution of HDO of phenol is shown in Fig. 8c. At a low temperature of 80°C and 12 bar H_2, the Ru/Nb_2O_5-100C18PA catalyst has ultra-high activity and selectivity for the hydrogenation of the benzene ring in phenol in monophasic and biphasic systems. The ratio of decalin to water can further affect the catalytic performance of the emulsion through the state and properties of the emulsion droplets formed. Consequently, the ratio of decalin to water needs to be refined to achieve the highest yield of cyclohexanol. When the ratio of decalin to water is 7.5/2.5, the conversion of phenol and the selectivity to cyclohexanol reaches the maximum value. This is due to the "solvent cage effect"[36,58]. Phenol molecules are surrounded by the catalyst in the solvent cage at the oil-water interface of the emulsion droplets. At the same time, the solubility of phenol in water is greater than that in decalin, so phenol is in water-in-oil (W/O) emulsions. The concentration in the droplets is higher, so that the phenol molecules in the solvent cage and the molecules in the main decalin solvent collide more frequently, thus giving the highest phenol conversion and cyclohexanol selectivity when the ratio of decalin to water is 7.5/2.5. At the same time, while the solubility of phenol in water is greater than that in decalin, the concentration of phenol in the droplets of the water-in-oil (W/O) emulsion is higher, making the phenol molecules in the solvent cage collide with each other more frequently than the molecules in the host decalin solvent, which gives the highest phenol conversion and cyclohexanol selectivity at a decalin to water ratio of 7.5/2.5. When the ratio of decalin to water gradually decreased, the conversion also decreased, but the selectivity to cyclohexanol remained basically unchanged, which may be caused by the expansion of the emulsion droplet size or the conversion of the system to an oil-in-water (O/W) emulsion as the proportion of water increased[59].

The polar monophasic water solvent and the non-polar monophasic decalin solvent also play an important role in product distribution. In the monophasic solvent decalin, the conversion of phenol is higher than that in the monophasic water solvent, which may be attributed to the lower solubility of H_2 in water[38,60]. Nevertheless, the monophasic decalin solvent showed the lowest selectivity to cyclohexanol compared with other solvents in different ratios, and more cyclohexanone and cyclohexane by-products are produced. In contrast, in the presence of polar water, whether in a

Green Chemistry Accepted Manuscript

This journal is © The Royal Society of Chemistry 20xx

View Article Online
DOI: 10.1039/D1GC04046D

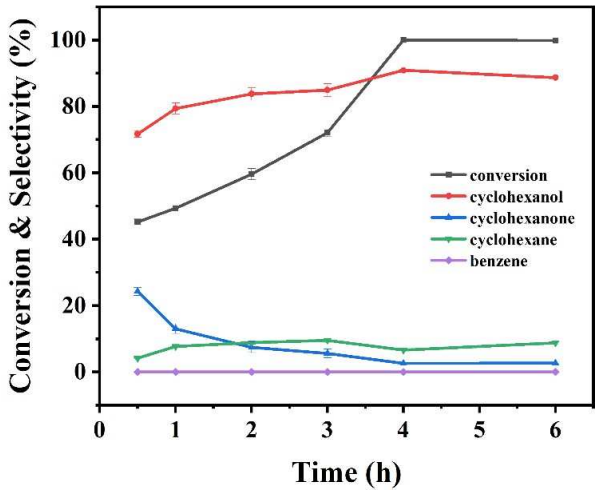

Fig. 9 Product distributions for the hydrogenation of phenol in the biphasic system over the Ru/Nb_2O_5-100C18PA catalyst versus the time. Reaction conditions: Phenol (0.05 g), Ru/Nb_2O_5-100C18PA (0.05 g), 12 bar H_2, decalin/water = 7.5 mL/2.5 mL, 80 °C.

Table 1 Hydrogenation of the intermediate products over the Ru/Nb_2O_5-100C18PA catalyst in biphasic system

Entry	Feed materials	Conversion (wt.%)	Selectivity (C mol%)			
1		93.7	0	0.1	99.9	-
2		2.4	0	4.5	-	95.5
3		91.5	-	100	-	-

Reaction conditions: Phenol (0.05 g), Ru/Nb_2O_5-100C18PA (0.05 g), decalin/water = 7.5 mL/2.5 mL, 12 bar H_2, 80 °C, 4 h.

monophasic water system or in a biphasic water and decalin system, other by-products were produced less, and the selectivity to cyclohexanol is also relatively high. This confirms that water plays a vital role in the phenol HDO reaction, which may be due to the interaction between the supported Ru catalyst and water, reducing the activation energy barrier and making the hydrogenation route easier[61]. The increase in the proton diffusion coefficient in water is also conducive to achieving a faster reaction rate[62].

3.4 Catalytic mechanism

3.4.1 Kinetics analysis. In order to further explore the internal reaction pathways and closely monitor the intermediate products, the kinetic behavior of phenol on the Ru/Nb_2O_5-100C18PA catalyst was run in a decalin/water biphasic system at 80°C for up to 6 hours, and the relationship between product distribution and time are shown in Fig. 9. With an extension of the reaction time, the phenol was converted entirely. The selectivity to cyclohexanone reached the highest value after the reaction time of 0.5 h and then gradually decreased. Meanwhile, the selectivity to cyclohexanol starting from

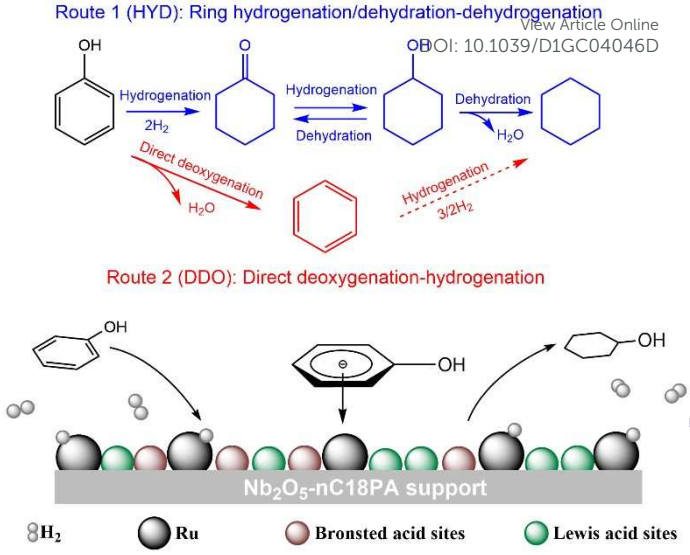

Scheme 1 Proposed reaction pathway of HDO of phenol in biphasic system and the mechanism of phenol to cyclohexanol over the Ru/Nb_2O_5-nC18PA catalyst.

0.5 h, gradually increased with time until it reached 93%. The results indicate that cyclohexanone is an intermediate product and can be converted into cyclohexanol as the reaction time increases. To further understand the hydrogenation of the benzene ring in phenol, cyclohexanone, cyclohexanol and benzene were used as probe reactants to carry out the conversion under the same conditions as phenol HDO (see Table 1). There was a pronounced difference in the conversion of cyclohexanol and cyclohexanone. Cyclohexanone was essentially converted to cyclohexanol, and only a minimal small amount of cyclohexane was formed. Conversion of cyclohexanol was very low at about 2%. In particular, almost all of the reacted cyclohexanol was converted to cyclohexanone, and the selectivity to cyclohexane was only 4.5%, indicating that cyclohexanone and cyclohexanol were reversible reactions and can be converted into each other. Still the conversion of cyclohexanol to cyclohexanone was very difficult and not easy to react. It is possible that the P-OH on the surface of the catalyst can combine with water to form an H-bond to inhibit the dehydration of cyclohexanol[63,64]. With benzene as a probe reaction the cyclohexane yield was about 91%, indicating that the catalyst acted on the benzene ring of phenol to achieve high-efficiency and selective conversion of cyclohexanol. Therefore, according to the results, phenol initially tends to produce cyclohexanone, and then cyclohexanone is further hydrogenated to form cyclohexanol, after which there is also a small conversion of cyclohexanol to cyclohexanone.

3.4.2 Reaction mechanism. To clarify the mechanism of the efficient conversion of cyclohexanol on the Ru/Nb_2O_5-100C18PA catalyst in the HDO of phenol in the biphasic system, the effect of not adding catalyst and adding a single catalyst with Nb_2O_5 support or Nb_2O_5-100C18PA support without Ru on the conversion of phenol to HDO were compared (Table 2, entry1, entry 2, entry 3). When the catalyst was not added, the conversion of phenol was 33.0%. The results indicate that the biphasic solvent of decalin and water in the catalytic system may interact with the reaction material, which may

Published on 13 December 2021. Downloaded by University of York on 12/15/2021 10:04:11 AM.

Green Chemistry Accepted Manuscript

View Article Online
DOI: 10.1039/D1GC04046D

Table 2 Hydrogenation of phenol over the different catalysts in biphasic system

Entry	Catalysts	Conversion (wt.%)	Selectivity (C mol%)			
1	-	33.0	0	1.12	61.4	37.4
2	Nb_2O_5	31.7	0	0.9	58.0	41.1
3	Nb_2O_5-100C18PA	26.0	0	2.3	65.3	32.4
4	Ru/Nb_2O_5-100C18PA	100.0	0	3.2	93.0	3.8
5	Ru/Nb_2O_5-100C18PA*	5.8	0	0	70.9	29.1

Reaction conditions: Phenol (0.05 g), Ru/Nb_2O_5-100C18PA (0.05 g), decalin/water = 7.5 mL/2.5 mL, 12 bar H_2, 80 °C, 4 h
* Other conditions are the same without H_2 pressure

be related to the polarity of water or decalin, phenol or the intermediates produced, and the solubility of the products[34,56,65,66], indicating that decalin and water may directly participate in the reaction[67,68]. When Nb_2O_5 and Nb_2O_5-100C18PA catalysts were added, there was 31.7% and 26.0% phenol conversion, respectively. The activity and selectivity of the Ru/Nb_2O_5-100C18PA catalyst was significantly improved compared with the others. Moreover, Fig. 9 shows that the cyclohexanone intermediate was formed first, indicating the high selectivity of benzene ring hydrogenation, implying the strong binding of the benzene ring to the catalyst surface and the high catalytic activity of the Ru/Nb_2O_5-100C18PA catalyst[27], which may have planar adsorption on the benzene ring in the phenol molecule[55,69].The hydrophilic-hydrophobic balance of the Ru catalyst in the biphasic system (the loading ratio of C18PA on the Nb_2O_5 support) plays a critical role in adjusting the selectivity of phenol HDO to cyclohexanol. In addition, the Ru nanoparticles are well dispersed on the catalyst. The amphiphilic nature of the Nb_2O_5-100C18PA composite made these catalysts preferentially separate at the water and oil interface rather than dispersed in either bulk phase, which can stabilize the emulsion and enhance the solvent mass transfer between different molecules in the solvent. Moreover, the biphasic catalytic process can promote the separation of hydrophobic molecules from the aqueous phase. Based on the difference in solubility in the liquid phase, these molecules can be selectively converted in only one of the liquid phases (i.e., phase selectivity). The separation of compounds into decalin with different polarities and aqueous solvent layers alleviates fragment repolymerization. As a result, high cyclohexanol yields can be obtained with less carbon build-up.

In summary, the excellent performance of the Ru/Nb_2O_5-100C18PA catalyst for the selective production of cyclohexanol from phenol is derived from its strong affinity for phenol, the planar adsorption of the benzene ring on phenol, and the biphasic catalysis and synergistic effect between Ru and Nb_2O_5-100C18PA composite support, result in high phenol conversion and cyclohexanol selectivity. Entry 5 of Table 5 compares the conversion of phenol HDO reaction at 5.8% when there was no hydrogen pressurization, indicating that the hydrogen pressure had the most significant effect on the HDO reaction. Here, based on the above research, we propose the overall reaction pathway of phenol HDO in the biphasic catalysis process in Scheme 1. Due to the strong affinity of Ru/Nb_2O_5-100C18PA catalyst to phenol, phenol is adsorbed onto the catalyst in a planar manner. At low temperatures (40°C-120°C), the temperature cannot reach the energy of Caryl-OH bond cleavage, inhibiting deoxygenation, so benzene does not undergo conversion during this process, phenol only undergoes the HYD path (route 1), and this reaction is generally a fast step. First, cyclohexanone was formed by hydrogenation of the benzene ring on phenol, and then cyclohexanone was further hydrogenated to form cyclohexanol. At present, only a small amount of cyclohexanol could in turn generate cyclohexanone or continue to react to generate cyclohexane. Among them, the hydrogenation of cyclohexanone to cyclohexanol was the main reaction process, and the yield of cyclohexanol was as high as 93.7% (Table 1, entry 1). At medium to high temperature intervals (140°C-220°C), phenol HDO undergoes two reaction pathways, as the DDO pathway and the HYD pathway (Scheme 1). Phenol directly deoxygenates to form benzene by breaking the $C_{aromatic}$-O bond (DDO pathway, route 2), which is mainly attributed to the activation of the C_{aryl}-O bond on the NbO_x species to reduce its bond energy[27], and is followed by a small conversion of benzene to cyclohexane (Table 1, entry 3). Meanwhile, phenol undergoes sequential hydrogenation in the HYD pathway, which mainly produces cyclohexanol. In addition, the DDO pathway dominates with increasing temperature and the yield of benzene keeps increasing to the detriment of cyclohexanol production.

3.5 Recyclability of the catalysts

The recyclability and stability of the catalyst are important indicators for evaluating heterogeneous (heterogeneous) catalysts. Fig. 10 shows the results of the catalytic activity test of the Ru/Nb_2O_5-100C18PA catalyst for multiple continuous operations. The results demonstrate that the Ru/Nb_2O_5-100C18PA catalyst can be successfully recycled five times while maintaining good activity. The

Published on 13 December 2021. Downloaded by University of York on 12/15/2021 10:04:11 AM.

Green Chemistry Accepted Manuscript

This journal is © The Royal Society of Chemistry 20xx

View Article Online
DOI: 10.1039/D1GC04046D

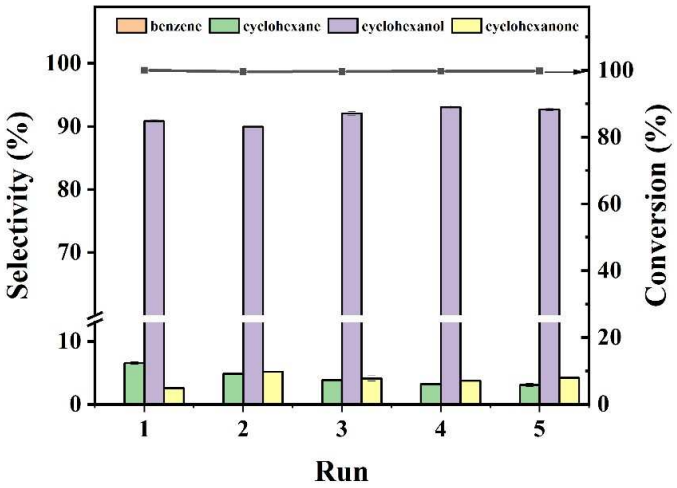

Fig. 10 Recycle of the catalyst. Reaction conditions: Phenol (0.05 g), Ru/Nb_2O_5-100C18PA (0.05 g), decalin/water = 7.5 mL/2.5 mL, 12 bar H_2, 80 °C, 4 h.

conversion of phenol was complete and the selectivity to cyclohexanol was basically unchanged, remaining within the range of 90-93%. The yield of other products was almost consistent. It is noteworthy that in the oil-water biphasic system, the catalyst can be arranged in one phase, and the recycling of the catalyst can be realized through simple phase separation, preventing the loss of catalyst activity and selectivity[70].

4. Conclusions

In this work, a Ru/Nb_2O_5-nC18PA catalyst was used to convert phenol to cyclohexanol in a decalin/water biphasic system. The synergy between the Ru nanoparticle catalyst and the Nb_2O_5-nC18PA support promotes the HDO of phenol. The metal Ru particles catalyzes the hydrogenation reaction, and the Nb_2O_5-nC18PA support promotes the strong bonding of the benzene ring to the catalyst surface and its planar adsorption. The dominance of the Lewis acid in the catalyst leads to the activation of the aromatic ring to produce cyclohexanol. The tunable wettability of the Nb_2O_5-nC18PA supports was a key factor in the formation of emulsions in the decalin/biphasic system. Process conditions such as reaction temperature, hydrogen partial pressure and reaction time have significant effects on the conversion of phenol and the selectivity to cyclohexanol. For the HDO of phenol, generally speaking, lower temperature, relatively lower hydrogen partial pressure and longer reaction time promote the hydrogenation of the benzene ring in phenol to cyclohexanol in the biphasic catalysis process. At 80 °C, 12 bar H_2, the Ru/Nb_2O_5-100C18PA catalyst achieved complete conversion of phenol and 93% cyclohexanol yield after 4h in the biphasic catalytic process using decalin and water. In general, the biphasic catalytic system is quite suitable for the hydrogenation of phenol to produce cyclohexanol. It is expected that it can be further extended to the hydrogenation of lignin-derived phenols to produce cyclohexanol, thus enhancing the value of lignin within biorefineries.

Author Contributions

Jiahui Zhan: Conceptualization, Methodology, Validation, Formal analysis, Investigation, Writing – original draft, Visualization. Rui Hu: Formal analysis, Writing – review & editing. Xi Luo: Investigation, Validation. Cheng Zhang: Conceptualization, Methodology, Writing – original draft, Writing – review & editing, Visualization. Gang Luo: Writing – review & editing, Validation. Jiajun Fan: Writing – review & editing, Validation. James H. Clark: Writing – review & editing, Validation. Shicheng Zhang: Conceptualization, Writing – review & editing, Supervision, Project administration, Funding acquisition.

Conflicts of interest

There are no conflicts to declare.

Acknowledgements

This research was supported by the National Natural Science Foundation of China (No. 21876030). We thank the reviewers for their positive and constructive comments.

References

1 Y. Liao, S.-F. Koelewijn, G. van den Bossche, J. van Aelst, S. van den Bosch, T. Renders, K. Navare, T. Nicolaï, K. van Aelst, M. Maesen, H. Matsushima, J. M. Thevelein, K. van Acker, B. Lagrain, D. Verboekend and B. F. Sels, *Science*, 2020, **367**, 1385.
2 J. Yan, Q. Meng, X. Shen, B. Chen, Y. Sun, J. Xiang, H. Liu and B. Han, *Science Advances*, 2020, **6**, eabd1951.
3 C. Li, X. Zhao, A. Wang, G. W. Huber and T. Zhang, *Chemical Reviews*, 2015, 115, 11559–11624.
4 A. J. Ragauskas, G. T. Beckham, M. J. Biddy, R. Chandra, F. Chen, M. F. Davis, B. H. Davison, R. A. Dixon, P. Gilna, M. Keller, P. Langan, A. K. Naskar, J. N. Saddler, T. J. Tschaplinski, G. A. Tuskan and C. E. Wyman, *Science*, 2014, **344**, 1246843.
5 S. Gillet, M. Aguedo, L. Petitjean, A. R. C. Morais, A. M. da Costa Lopes, R. M. Łukasik and P. T. Anastas, *Green Chemistry*, 2017, 19, 4200–4233.
6 H. Wang, J. Male and Y. Wang, *ACS Catalysis*, 2013, 3, 1047–1070.
7 H. Xia, H. Tan, H. Cui, F. Song, Y. Zhang, R. Zhao, Z. N. Chen, W. Yi and Z. Li, *Catalysis Science and Technology*, 2021, **11**, 1881–1887.
8 Y. Xiang, L. Ma, C. Lu, Q. Zhang and X. Li, *Green Chemistry*, 2008, **10**, 939–94.
9 J. Long, S. Shu, Q. Wu, Z. Yuan, T. Wang, Y. Xu, X. Zhang, Q. Zhang and L. Ma, *Energy Conversion and Management*, 2015, **105**, 570–577.
10 Z. Song, D. Ren, T. Wang, F. Jin, Q. Jiang and Z. Huo, *Catalysis Today*, 2016, **274**, 94–98.
11 S. S. Wong, R. Shu, J. Zhang, H. Liu and N. Yan, *Chemical Society Reviews*, 2020, 49, 5510–5560.
12 Y. Xu, Z. Peng, Y. Yu, D. Wang, J. Liu, Q. Zhang and C. Wang, *New Journal of Chemistry*, 2020, **44**, 5088–5096.
13 F. Yang, D. Liu, Y. Zhao, H. Wang, J. Han, Q. Ge and X. Zhu, *ACS Catalysis*, 2018, **8**, 1672–1682.
14 J. Zhong, J. Chen and L. Chen, *Catalysis Science and Technology*, 2014, 4, 3555–3569.

Published on 13 December 2021. Downloaded by University of York on 12/15/2021 10:04:11 AM.

Green Chemistry Accepted Manuscript

View Article Online
DOI: 10.1039/D1GC04046D

15 M. Saidi, F. Samimi, D. Karimipourfard, T. Nimmanwudipong, B. C. Gates and M. R. Rahimpour, *Energy and Environmental Science*, 2014, 7, 103–129.

16 S. Dai, Z. Hou, M. Chen, Y. Cui, W. Qian, Q. Peng, J. Wang, H. Gong and J. Fang, *Langmuir*, 2020, **36**, 11589–11599.

17 X. Wang, M. Arai, Q. Wu, C. Zhang and F. Zhao, *Green Chemistry*, 2020, **22**, 8140–8168.

18 T. Cordero-Lanzac, R. Palos, I. Hita, J. M. Arandes, J. Rodríguez-Mirasol, T. Cordero, J. Bilbao and P. Castaño, *Applied Catalysis B: Environmental*, 2018, **239**, 513–524.

19 L. Wang, J. Zhang, X. Yi, A. Zheng, F. Deng, C. Chen, Y. Ji, F. Liu, X. Meng and F. S. Xiao, *ACS Catalysis*, 2015, **5**, 2727–2734.

20 D. Liu, G. Li, F. Yang, H. Wang, J. Han, X. Zhu and Q. Ge, *Journal of Physical Chemistry C*, 2017, **121**, 12249–12260.

21 W. Zhang, J. Chen, R. Liu, S. Wang, L. Chen and K. Li, *ACS Sustainable Chemistry and Engineering*, 2014, **2**, 683–691.

22 A. Li, K. Shen, J. Chen, Z. Li and Y. Li, *Chemical Engineering Science*, 2017, **166**, 66–76.

23 V. Vinokurov, A. Glotov, Y. Chudakov, A. Stavitskaya, E. Ivanov, P. Gushchin, A. Zolotukhina, A. Maximov, E. Karakhanov and Y. Lvov, *Industrial and Engineering Chemistry Research*, 2017, **56**, 14043–14052.

24 W. Luo, W. Cao, P. C. A. Bruijnincx, L. Lin, A. Wang and T. Zhang, *Green Chemistry*, 2019, **21**, 3744–3768.

25 M. Chatterjee, T. Ishizaka, A. Suzuki and H. Kawanami, *Chemical Communications*, 2013, **49**, 4567–4569.

26 Y. Jing, Y. Wang, S. Furukawa, J. Xia, C. Sun, M. J. Hülsey, H. Wang, Y. Guo, X. Liu and N. Yan, *Angewandte Chemie - International Edition*, 2021, **60**, 5527–5535.

27 Y. Shao, Q. Xia, L. Dong, X. Liu, X. Han, S. F. Parker, Y. Cheng, L. L. Daemen, A. J. Ramirez-Cuesta, S. Yang and Y. Wang, *Nature Communications*, 2017, **8**, 16104.

28 C. Sievers, Y. Noda, L. Qi, E. M. Albuquerque, R. M. Rioux and S. L. Scott, *ACS Catalysis*, 2016, **6**, 8286–8307.

29 A. H. Jenkins, C. B. Musgrave and J. W. Medlin, *ACS Applied Materials and Interfaces*, 2019, **11**, 41289–41296.

30 P. Hao, D. K. Schwartz and J. W. Medlin, *ACS Catalysis*, 2018, **8**, 11165–11173.

31 P. D. Coan, L. D. Ellis, M. B. Griffin, D. K. Schwartz and J. W. Medlin, *Journal of Physical Chemistry C*, 2018, **122**, 6637–6647.

32 T. van Cleve, D. Underhill, M. Veiga Rodrigues, C. Sievers and J. W. Medlin, *Langmuir*, 2018, **34**, 3619–3625.

33 J. Zhang, L. D. Ellis, B. Wang, M. J. Dzara, C. Sievers, S. Pylypenko, E. Nikolla and J. W. Medlin, *Nature Catalysis*, 2018, **1**, 148–155.

34 S. Crossley, J. Faria, M. Shen and D. E. Resasco, *Science*, 2010, **327**, 68.

35 K. M. Isa, T. A. T. Abdullah and U. F. M. Ali, *Renewable and Sustainable Energy Reviews*, 2018, 81, 1259–1268.

36 C. Zhang, C. Jia, Y. Cao, Y. Yao, S. Xie, S. Zhang and H. Lin, *Green Chemistry*, 2019, **21**, 1668–1679.

37 M. Memari and N. Memarian, *Journal of Materials Science: Materials in Electronics*, 2020, **31**, 2298–2307.

38 G. Jiang, Y. Hu, G. Xu, X. Mu and H. Liu, *ACS Sustainable Chemistry and Engineering*, 2018, **6**, 5772–5783.

39 D. Rochefort, P. Dabo, D. Guay and P. M. A. Sherwood, *Electrochimica Acta*, 2003, **48**, 4245–4252.

40 N. Wang, W. Qian, W. Chu and F. Wei, *Catalysis Science and Technology*, 2016, **6**, 3594–3605.

41 H. Huang, Q. Dai and X. Wang, *Applied Catalysis B: Environmental*, 2014, **158–159**, 96–105.

42 Y. Zheng, N. Zhao and J. Chen, *Applied Catalysis B: Environmental*, 2019, **250**, 280–291.

43 S. Furukawa, Y. Matsunami, I. Hamada, Y. Hashimoto, Y. Sato and T. Komatsu, *ACS Catalysis*, 2018, **8**, 8177–8181.

44 C. H. Lien and J. W. Medlin, *Journal of Catalysis*, 2016, **339**, 38–46.

45 R. Luschtinetz, A. F. Oliveira, H. A. Duarte and G. Seifert, *Zeitschrift fur Anorganische und Allgemeine Chemie*, 2010, **636**, 1506–1512.

46 D. Ni, L. Wang, Y. Sun, Z. Guan, S. Yang and K. Zhou, *Angewandte Chemie - International Edition*, 2010, **49**, 4223–4227.

47 J. J. Max and C. Chapados, *Journal of Physical Chemistry A*, 2004, **108**, 3324–3337.

48 H. Liu, T. Jiang, B. Han, S. Liang and Y. Zhou, *Science*, 2009, **326**, 1250.

49 R. R. Deshmukh, J. W. Lee, U. S. Shin, J. Y. Lee and C. E. Song, *Angewandte Chemie - International Edition*, 2008, **47**, 8615–8617.

50 F. F. Sene, J. R. Martinelli and L. Gomes, in *Journal of Non-Crystalline Solids*, Elsevier, 2004, vol. 348, pp. 30–37.

51 C. A. Teles, P. M. de Souza, A. H. Braga, R. C. Rabelo-Neto, A. Teran, G. Jacobs, D. E. Resasco and F. B. Noronha, *Applied Catalysis B: Environmental*, 2019, **249**, 292–305.

52 H. Y. T. Chen and G. Pacchioni, *ChemCatChem*, 2016, **8**, 2492–2499.

53 C. A. Teles, P. M. de Souza, R. C. Rabelo-Neto, M. B. Griffin, C. Mukarakate, K. A. Orton, D. E. Resasco and F. B. Noronha, *Applied Catalysis B: Environmental*, 2018, **238**, 38–50.

54 X. Liu, W. Jia, G. Xu, Y. Zhang and Y. Fu, *ACS Sustainable Chemistry and Engineering*, 2017, **5**, 8594–8601.

55 Z. Luo, Z. Zheng, Y. Wang, G. Sun, H. Jiang and C. Zhao, *Green Chemistry*, 2016, **18**, 5845–5858.

56 Z. Zhu, H. Tan, J. Wang, S. Yu and K. Zhou, *Green Chemistry*, 2014, **16**, 2636–2643.

57 C. Chen, G. Chen, F. Yang, H. Wang, J. Han, Q. Ge and X. Zhu, *Chemical Engineering Science*, 2015, **135**, 145–154.

58 C. Li, H. Cai, B. Zhang, W. Li, G. Pei, T. Dai, A. Wang and T. Zhang, *Cuihua Xuebao/Chinese Journal of Catalysis*, 2015, **36**, 1638–1646.

59 M. Shen and D. E. Resasco, *Langmuir*, 2009, **25**, 10843–10851.

60 X. Yang, Y. Liang, Y. Cheng, W. Song, X. Wang, Z. Wang and J. Qiu, *Catalysis Communications*, 2014, **47**, 28–31.

61 C. Michel and P. Gallezot, *ACS Catalysis*, 2015, 5, 4130–4132.

62 B. S. Akpa, C. D'Agostino, L. F. Gladden, K. Hindle, H. Manyar, J. McGregor, R. Li, M. Neurock, N. Sinha, E. H. Stitt, D. Weber, J. A. Zeitler and D. W. Rooney, *Journal of Catalysis*, 2012, **289**, 30–41.

63 Z. Yu, Y. Wang, Z. Sun, X. Li, A. Wang, D. M. Camaioni and J. A. Lercher, *Green Chemistry*, 2018, **20**, 609–619.

64 E. Tang, D. di Tommaso and N. H. de Leeuw, *The Journal of Chemical Physics*, 2009, **130**, 234502.

65 M. Wang, Y. Zhao, D. Mei, R. M. Bullock, O. Y. Gutiérrez, D. M. Camaioni and J. A. Lercher, *Angewandte Chemie*, 2020, **132**, 1461–1465.

66 C. Zhao, Y. Kou, A. A. Lemonidou, X. Li and J. A. Lercher, *Angewandte Chemie - International Edition*, 2009, **48**, 3987–3990.

Published on 13 December 2021. Downloaded by University of York on 12/15/2021 10:04:11 AM.

Green Chemistry Accepted Manuscript

This journal is © The Royal Society of Chemistry 20xx

Please do not adjust margins

View Article Online
DOI: 10.1039/D1GC04046D

67 R. C. Nelson, B. Baek, P. Ruiz, B. Goundie, A. Brooks, M. C. Wheeler, B. G. Frederick, L. C. Grabow and R. N. Austin, *ACS Catalysis*, 2015, **5**, 6509–6523.
68 T. O. Omotoso, B. Baek, L. C. Grabow and S. P. Crossley, *ChemCatChem*, 2017, **9**, 2642–2651.
69 L. Dong, L. Lin, X. Han, X. Si, X. Liu, Y. Guo, F. Lu, S. Rudić, S. F. Parker, S. Yang and Y. Wang, *Chem*, 2019, **5**, 1521–1536.
70 M. Schmidt, T. Pogrzeba, L. Hohl, A. Weber, A. Kielholz, M. Kraume and R. Schomäcker, *Molecular Catalysis*, 2017, **439**, 1–8.

Published on 13 December 2021. Downloaded by University of York on 12/15/2021 10:04:11 AM.

Green Chemistry Accepted Manuscript

Please do not adjust margins